Structure of an anti-Lewis X Fab fragment in complex with its Lewis X antigen

Roon, A.M.; Pannu, N.S.; Vrind, J.P.; Marel, G.A. van der; Boom, J.H. van; Hokke, C.H.; ... ; Abrahams, J.P.

Structure, Vol. 12, 1227–1236, July, 2004, ©2004 Elsevier Ltd. All rights reserved. DOI 10.1016/j.str.2004.05.008

Structure of an Anti-Lewis X Fab Fragment in Complex with Its Lewis X Antigen

Anne-Marie M. van Roon,[1,3] Navraj S. Pannu,[1] Johannes P.M. de Vrind,[1] Gijs A. van der Marel,[2] Jacques H. van Boom,[2] Cornelis H. Hokke,[3] André M. Deelder,[3] and Jan Pieter Abrahams[1,*]

[1]Department of Biophysical Structural Chemistry
[2]Department of Bio-Organic Synthesis
Leiden University
P.O. Box 9502
2300 RA, Leiden
The Netherlands
[3]Department of Parasitology
Leiden University Medical Center
P.O. Box 9600
2300 RC, Leiden
The Netherlands

Summary

The Lewis X trisaccharide is pivotal in mediating specific cell-cell interactions. Monoclonal antibody 291-2G3-A, which was generated from mice infected with schistosomes, has been shown to recognize the Lewis X trisaccharide. Here we describe the structure of the Fab fragment of 291-2G3-A, with Lewis X, to 1.8 Å resolution. The crystallographic analysis revealed that the antigen binding site is a rather shallow binding pocket, and residues from all six complementary determining regions of the antibody contact all sugar residues. The high specificity of the binding pocket does not result in high affinity; the K_D determined by isothermal calorimetry is 11 μM. However, this affinity is in the same range as for other sugar-antibody complexes. The detailed understanding of the antibody-Lewis X interaction revealed by the crystal structure may be helpful in the design of better diagnostic tools for schistosomiasis and for studying Lewis X-mediated cell-cell interactions by antibody interference.

Introduction

The trisaccharide Lewis X (Le^x, Galβ1-4(Fucα1-3) GlcNAcβ) is one of the histo-blood group carbohydrate determinants and is expressed by higher organisms in various tissues, such as brain, kidney, and stomach (Fox et al., 1983), where it is thought to play an important role in cell-cell adhesion. Le^x has been detected on numerous different tumor cells (Hakomori, 1984, 2000), and it also plays an important role in the immunology of schistosomiasis, a parasitic disease that affects hundreds of millions of people in the tropics. Throughout the different life cycle stages of the parasite, Le^x and other carbohydrates are abundantly expressed on its outer membrane or excreted into the circulation of the host (Hokke and Deelder, 2001; and references cited therein). The parasite differentially expresses Le^x on glycolipids and glycoproteins, both in monomeric and in multimeric form (Huang et al., 2001; Khoo et al., 2001; Koster and Strand, 1994; Srivatsan et al., 1992; Van Remoortere et al., 2000; Weiss and Strand, 1985; Wuhrer et al., 2000). For example, polymeric Le^x is expressed as the major immunogenic part of the gut-associated circulating cathodic antigen (CCA) (Van Dam et al., 1994). This antigen is excreted into the circulation of the host by the adult worms in abundant amounts, allowing sensitive immunodiagnostic detection of schistosomiasis (De Jonge et al., 1990). Le^x-containing glycoconjugates have been shown to stimulate B cells to proliferate and to produce factors that downregulate the T_H1 immune response and upregulate the T_H2 immune response (Velupillai and Harn, 1994; Velupillai et al., 2000). Individuals suffering from schistosomiasis mount an immune response against Le^x (Nyame et al., 1996, 1997; Richter et al., 1996; Van Remoortere et al., 2001). Antibodies to the Le^x-containing glycans have been reported to mediate complement-dependent cytolysis in vitro of human granulocytes (Van Dam et al., 1996), suggesting a mechanism for the mild neutropenia sometimes observed during a schistosome infection (Borojevic et al., 1983). Recent studies have shown that Le^x in different oligomeric states gives rise to the elicitation of different groups of anti-Le^x antibodies (Van Remoortere et al., 2003; van Roon et al., 2004). To further understand the basis of the specificity of these antibodies for Le^x, we performed an X-ray crystallographic analysis of monoclonal antibody (mAb) 291-2G3-A that binds monomeric, dimeric, and trimeric Le^x to gain detailed structural insight in the protein-Le^x interaction. Le^x, anti-Le^x antibodies, and carbohydrate binding proteins (lectins) that recognize Le^x are involved in the activation of the immune system during a schistosomal infection. Therefore, this information will aid in the rational design of better diagnostics for schistosomiasis and could also be helpful for the development of new intervention tools.

Previously, structures of bacterial carbohydrates in complex with a Fab fragment have been solved (Cygler et al., 1991; Nguyen et al., 2003; Villeneuve et al., 2000; Vyas et al., 2002; Zdanov et al., 1994). Recently the structures of a Fab fragment bound to a disaccharide and an oligosaccharide present on the gp120 envelope glycoprotein from human immunodeficiency virus were reported (Calarese et al., 2003). Next to interactions with these oligosaccharides expressed by invading pathogens, there is considerable interest in the interactions of endogenous oligosaccharides with antibodies in view of the potential interference with cell-cell interactions and the immune system. The only example for which structural information is available is the complex of LewisY with a Fab fragment of an antitumor antibody (Jeffrey et al., 1995). Le^x is of particular interest as it is expressed both by schistosomes and by the host itself. Here we report the crystal structures of a Fab fragment with and without Le^x to 1.8 Å and 2.05 Å resolution, respectively.

*Correspondence: abrahams@chem.leidenuniv.nl

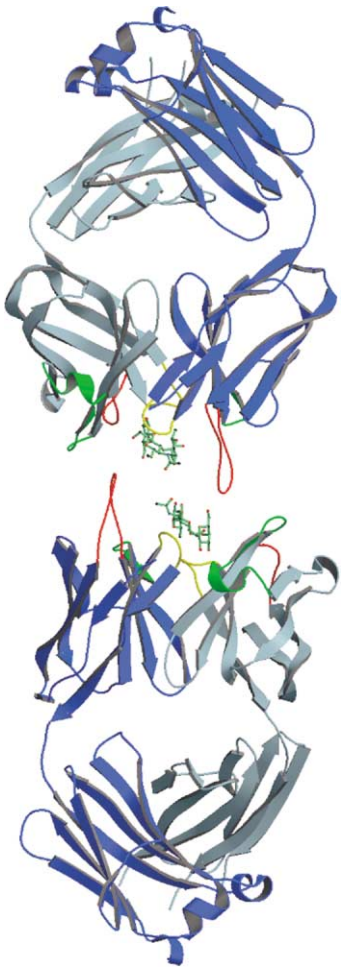

Figure 1. Structure of the Two Fab Fragments in Complex with Le^x Present in the Asymmetric Unit

The light chains are blue, the heavy chains are light blue, and Le^x is light green. Complementary determining regions L1 and H1 are red, L2 and H2 are green, and L3 and H3 are yellow. The picture was produced with the programs MOLSCRIPT (Kraulis, 1991) and Raster3D (Merritt and Bacon, 1997).

Results and Discussion

Overall Crystal Structure of the Fab Fragment

The structure of the Fab fragment of anti-Le^x mAb 291-2G3-A (IgG3, V_κ) has been solved with (Figure 1) and without its Le^x ligand with free R factors of 24.7% and 24.3%, respectively (Protein Data Bank codes 1UZ8 and 1UZ6, respectively). All residues of the Fab with Le^x are well ordered, except for amino acids 128–132 of the heavy chain, which form a flexible loop often disordered in Fab fragments. In the Fab without Le^x, in addition to the residues 128–132 of the heavy chain, residues 196–203 of the light chain were not visible, as they are also part of a flexible loop. Both structures have over 90% of the residues in the most favored region, having only Met L51 in the disallowed region. Crystallographic statistics are given in Table 1. Attempts to cocrystallize the Fab fragment with Le^x were unsuccessful; small impurities present in the Le^x solution as a result of the organic synthesis probably interfered with crystal nucleation by causing phase separation. Fortunately, the Le^x trisaccharide could be soaked into crystals of the Fab fragment; the likely reason for this is that the antigen binding sites of two Fabs point toward each other in the crystal, with a solvent channel running through the middle. This facilitates the diffusion of the ligand into the binding pocket of the Fab fragment to full occupancy and without damaging the crystal. There is no large conformational change upon binding of the sugar, which is well ordered in the crystal. Clear electron density is present in the binding site, in which Le^x could be nicely fitted (Figure 2). The elbow angle of the Fab fragments with and without Le^x are 140.6° and 134.7°, respectively; this small difference is most likely due to different crystal packing, as the crystals were grown under different crystallization conditions (van Roon et al., 2003).

The protein sequence of the Fab fragment was determined (Figure 3), and the structure and sequence of the six complementary determining regions (CDRs) were analyzed (Martin, 1996). CDR-L1, CDR-L2, and CDR-L3 belong to the classes 4/16A, 1/7A, and 1/9A, respectively, and CDR-H1 and CDR-H2 belong to the classes 1/10A and 3/10B, respectively. In the case of CDR-H3, the structure was predicted to be a kinked base (Morea et al., 1998; Shirai et al., 1996, 1999) on the basis of sequence rule i-c. This rule states that when residue n−1 is Asp (n is the number of residues of CDR-H3), residue 0 is basic, and residue −1 is not basic, the side chain of the Asp forms a salt bridge with the basic residue at the start of CDR-H3, which is typical for the kinked base. Although these residues can indeed be found in the sequence of CDR-H3, the structure forms an extended base (Figure 4), because the side chain of Asp H101 forms hydrogen bonds with the side chains of Trp H103 and Tyr L36 and the amide of Gly H97. Furthermore, three hydrogen bonds stabilizing the loop are present between Oγ1 of Thr H98 with the carbonyl of Glu H95, the amide of Arg 99H, and the amide of Phe 100H. In other structures, a basic residue at position L46 tends to form a salt bridge with Asp H101, thereby inducing the extended base structure, and also prolines in the β hairpin region can deform the structure into an extended base structure (for examples, see Morea et al., 1998; Shirai et al., 1996). These residues are not present in our structure however. A likely explanation for the formation of this extended structure is the presence of the charge and size of Arg H99 and Phe H100 in the hairpin region. The main chain is locally deformed, and the side chain of Arg H94 now forms a hydrogen bond with the carbonyl of Phe H100.

Fab Sugar Interaction

The Fab fragment forms a rather shallow binding pocket, which nicely accommodates the Le^x trisaccharide (Figure 5). The pocket is approximately 15 Å long, 13 Å wide, and 10 Å deep (distances were measured in Xtalview [Mcree, 1999]). Upon binding of Le^x, 302 $Å^2$ of the solvent-accessible surface of the Fab fragment is buried. Residues from all six CDRs contact the sugar, in contrast to other antibodies in which CDR-L2 rarely contributes to binding of the antigen (Wilson and Stanfield, 1993).

Table 1. Data Collection and Refinement Statistics

	291-2G3-A Fab Unliganded	291-2G3-A Fab with Lewis X
Data Collection		
Beamline	APS ID19	ESRF ID14-1
Wavelength (Å)	1.03	0.934
Spacegroup	P1	P1
Unit cell parameters a × b × c (Å)	67.4 × 71.6 × 104.8	45.1 × 60.8 × 91.6
α × β × γ (°)	86.5 × 71.3 × 83.3	96.0 × 95.4 × 101.78
Resolution (Å)[a]	45–2.05 (2.12–2.05)	45–1.8 (1.86–1.80)
Completeness (%)	88.1 (38.9)	92.9 (72.0)
Measured reflections	256292	951604
Unique reflections	103313	87852
R_{merge}[b]	4.6 (32.9)	9.4 (38.6)
Average I/σ (I)	19.7 (2.1)	11.1 (2.2)
Refinement		
R factor (%)	19.8 (27)	21.0 (25)
Free R factor (%)	24.3 (31)	24.7 (27)
No of TLS groups	56	28
No of Fabs in the asymmetric unit	4	2
No of protein residues	1628	826
No of solvent molecules	349	288
No of ions/ligands	4 sulfates	6 carbohydrate residues
Average total B value protein (Å^2)	53.2	46.0
Average total B value Le^x (Å^2)	—	51.1
Average total B value water (Å^2)	47.8	44.7
Validation		
Ramachandran plot (%)		
Most favored region	92.8	91.6
Additionally favored region	6.8	8.0
Generally allowed region	0.1	0.1
Disallowed region	0.3	0.3
Rmsd bonds (Å)	0.014	0.005
Rmsd angles (°)	1.14	1.15

[a] Values of reflections recorded in the highest resolution shell are shown in parentheses.
[b] $R_{merge} = \Sigma\ (|I - \langle I \rangle|)/\Sigma\ (I)$ (scalepack output).

Table 2 summarizes all the hydrogen bonds between the protein and the sugar residues. Hydrogen bonds usually contribute most to the stability of protein-sugar complexes. Amino acids having polar planar side chains are often highly abundant in binding pockets, as these residues can assist in the formation of stable hydrogen bond networks. Furthermore, aromatic residues like tyrosine and tryptophan play an important role in sugar binding since they are not only capable of forming hydrogen bonds with the sugar residues but can also stack with the hydrophobic face of the pyranoside rings (Quiocho, 1989). Indeed, most residues found in the binding site (Figure 3) that directly interact with Le^x have either polar or aromatic side chains (Figure 6), with only two hydrogen bonds formed by main chain atoms. In total, 11 hydrogen bonds are formed between sugar and protein residues.

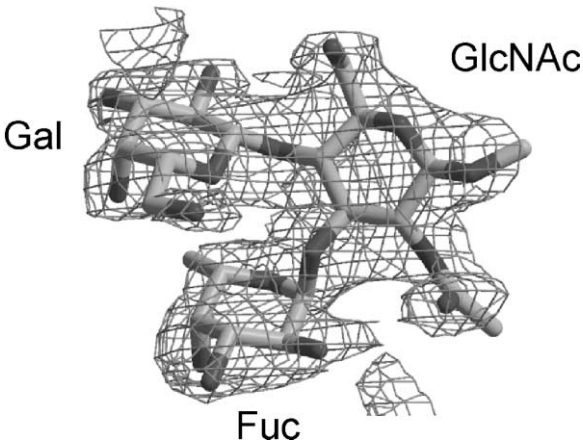

Figure 2. $2F_o - F_c$ Electron Density for Le^x Contoured at 1.2 σ
This picture was generated with Xtalview (Mcree, 1999).

Furthermore, three well ordered water molecules are found in the binding pocket bridging protein and sugar residues. Two water molecules interact with galactose (Gal) O2 and O3 and fit snugly in a polar binding pocket bridging CDR-H1, CDR-H2, and CDR-H3, maintaining a stable hydrogen bond network between these CDRs. The third water molecule bridges between fucose (Fuc) O4 and the carbonyl of Gly H97. The asymmetric unit contains two Fab-carbohydrate complexes, and only in one of them are the water molecules interacting with Gal O3 and Fuc O4 visible. Most likely, these water molecules are also present in the other Fab-sugar complex, but are perhaps more disordered or not fully occupied and therefore not visible. Overlaying the two structures shows no differences between the binding pockets

```
Light chain      10                  20     CDR-L1 27 a b c d e    30
D I V M T Q A A F S N P V T L G T S A S I S C R S S K S L L Y S N G I T
               40                  50   CDR-L2         60
Y L Y W Y L Q K P G Q S P Q L L I Y Q M S N L A S G V P D R F S S S G S
  70                 80                  90   CDR-L3         100
G T D F T L R I S R V E A E D V G V Y Y C A Q N L E V P W T F G G G T K
  106a
L E I K R A

Heavy chain      10                  20                  30 CDR-H1
E V K L L E S G G G L V Q P G G S Q K L S C A A S G F D F S G Y W M S W
    40                  50  52 a   CDR-H2     60                  70
V R Q A P G K G L E W I G E I N P D S S T I N Y T P S L K D K F I I S R
             80    82 a b c             90          CDR-H3 100
D N A K N T L Y L Q M S K V R S E D T A L Y Y C A R E T G T R F D Y W G
        110
Q G T T L T V S S
```

Figure 3. Sequence of Variable Light and Heavy Chains

Complementary determining regions are depicted in bold. Numbering is according to the Kabat numbering scheme and complementary determining regions (CDR; definitions according to the AbM definitions [http://www.bioinf.org.uk/abs]) (Martin, 1996).

(data not shown). The average total B factor for the protein, which includes the tls component used in the crystal structure refinement (Winn et al., 2001), is in the same range as the water molecules (Table 1).

An extensive hydrogen bond network is present around the binding pocket, helping to maintain the conformation of the binding pocket. The side chain of Glu H50 bridges the Gal and the *N*-acetylglucosamine methyl glycoside (Mag) and further stabilizes the complex. This residue also played a central role in the formation of a stable hydrogen network in the structure of a Fab fragment in complex with a bacterial carbohydrate (Vyas et al., 2002). One striking observation is that the rather long CDR-L1 loop (16 residues) inserts into the binding pocket of the other Fab fragment (Figure 1), interacting with its heavy chain via a hydrogen bond between ND2 of Asn B58 and the carbonyl of Ser L27e and binding with its sugar. The side chain hydroxyl group of Tyr A27d, located at the bottom of this loop, forms a bifurcated hydrogen bond with O1 and O7 of the Mag that is bound to the other Fab molecule in the unit cell. Furthermore, this tyrosine shields its own binding pocket by making a Van der Waals interaction with the methyl group of the acetyl function of the Mag residue that is bound to the same Fab molecule. The interaction between Tyr A27d and the Le^x bound to the other Fab fragment may not have biological relevance, but it does help stabilizing the Fab sugar complex in the crystal. The side chain of residue Gln L50, which is part of CDR-L2, makes a hydrogen bond with O4 of the fucose. This could be the reason why the main chain is slightly distorted at Met L51 according to the Ramachandran plot. This residue, however, fits very nicely into the electron density, suggesting that the conformation of CDR L2 is the cause of the distortion. Furthermore, Trp H33 forms an aromatic stacking interaction with a hydrophobic patch (C3, C5, and C6) on the β face of the galactose. This residue is stabilized by Oϵ1 of Glu H95 from CDR-H3 by forming a hydrogen bond with the main chain NH of Trp H33, and NH of Glu H95 donates a hydrogen bond to the carbonyl of Trp H33.

Comparison between the Bound and Unbound Structures

Upon binding of the sugar, the structure of the binding pocket of the Fab does not change except for the side chain of Gln L50, which changes slightly to make a favorable hydrogen bond with Fuc O4. Both the unliganded and the liganded structures have Met L51 in an unfavorable conformation.

The structure of unbound Le^x had been previously determined (Perez et al., 1996). The overall trisaccharide structure is similar to that in the Fab complex (Table 3), which is not very surprising considering the rather rigid

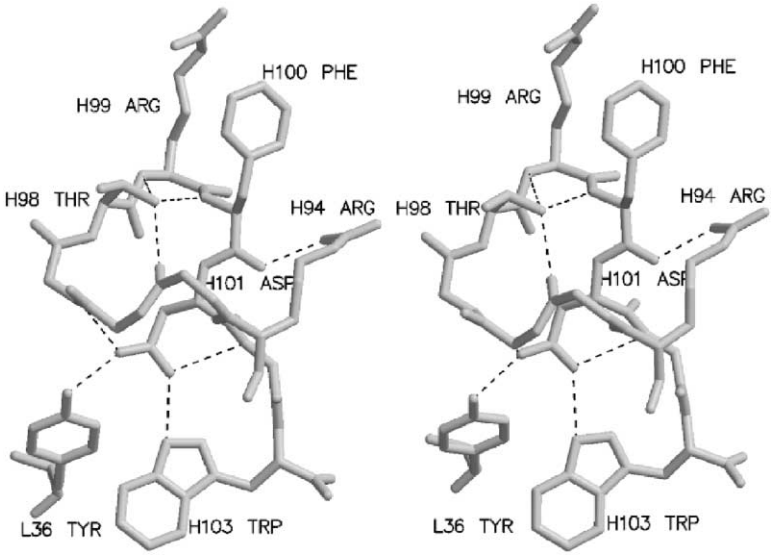

Figure 4. Stereoview of the CDR-H3 Loop

Asp H101 makes hydrogen bonds to the side chains of Trp H103 and Tyr L36, forming an extended base structure. The picture was produced with the programs MOLSCRIPT (Kraulis, 1991) and Raster3D (Merritt and Bacon, 1997).

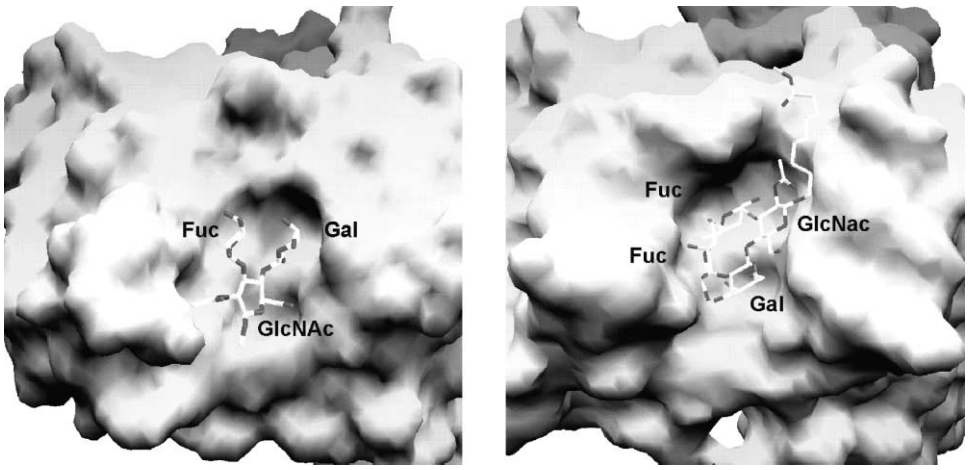

Figure 5. Comparison between the Binding Pocket of 291-2G3-A with Le^x and the Binding Pocket of mAb BR96 with Le^y Nonoate Methyl Ester

The binding pocket of 291-2G3-A with Le^x (left), and the binding pocket of mAb BR96 with Le^y nonoate methyl ester (right). It can immediately be seen that the both sugars have an opposite direction of binding with the Fabs. Both proteins are displayed as a surface representation. This picture was generated with GRASP (Nicholls et al., 1991).

structure of Le^x. There are, however, some striking differences. The Mag has a gauche-trans conformation in the Le^x crystals, which is an energetically favorable conformation (Wormald et al., 2002). However, bound to the protein, it adopts a gauche-gauche conformation, allowing a hydrogen bond with Glu H50. Furthermore, in Gal (which has a trans-gauche conformation in the Le^x crystals), the 6′-hydroxyl group is rotated to a gauche-trans conformation. Although in this conformation the primary hydroxyl group does not form a hydrogen bond, it is orientated parallel to the hydrophobic face of Trp H33 for optimal aromatic stacking.

Table 2. Hydrogen Bonds between Sugar and Protein or Water

	Fab Residue	Atom	Distance (Å)[a]
Mag Y			
O1	Tyr A27d	OH	3.02
O7	Tyr A27d	OH	3.25
N2	Asn L91	O	3.06
O4	Asn L91	ND2	2.97
O6	Glu H50	Oϵ2	2.46
Fuc Y			
O4	Gln L50	Oϵ1	2.91
O5	Asn L91	ND2	3.15
O4	HOH 242[b]		3.09
Gal Y			
O2	Glu H50	Oϵ1	2.71
O2	Trp L96	Nϵ1	2.90
O2	Thr H96	Oγ1	3.22
O3	Thr H96	N	3.22
O2	HOH 282[c]		3.13
O3	HOH 203[b]		2.77

[a] Hydrogen bonds between one Fab fragment and Le^x are presented; possible differences in distance between the atoms in the other Fab-Le^x complex present in the asymmetric unit fall outside the resolution range.

[b] These water molecules are absent in the other complex present in the asymmetric unit.

[c] Present as water molecule HOH 280 in the other complex.

Comparison with Anti-Le^y Fab BR96

The only other structure of a Fab fragment with a histo-blood group oligosaccharide is the crystal structure of a Fab fragment of mAb BR96 in complex with the nonoate methyl ester derivative of Lewis Y [Fucα1-2Galβ1-4(Fucα1-3)GlcNAcβ1-$(CH_2)_8COOCH_3$, nLe^y] (Jeffrey et al., 1995). Le^y is a tetrasaccharide containing a Le^x moiety. Interestingly, the overall geometry of the Le^x part of Le^y is, like the geometry of Le^x not bound to a protein, very comparable to Le^x bound to the 291-2G3-A (Table 3). Despite this similarity, the mode of binding of the sugars to the protein is very different. In the BR96 structure, the nonreducing end of Le^y points toward CDR-L1, CDR-L3, and CDR-H2, whereas Le^x in the 291-2G3-A structure sits almost 180° rotated in the binding pocket and is pointing toward CDR-H1 and CDR-H3 (Figure 5). Both antibodies represent a cavity-type antibody (Padlan and Kabat, 1991) and have a binding pocket that fits the complete sugar. In both complexes, all sugar residues are involved in binding. Moreover, it was found that BR96 does not interact with Le^x (Hellstrom et al., 1990). The binding pockets of both antibodies have approximately the same size. Upon binding of the sugars, Le^x buries 302 Å^2 of the solvent-accessible surface, whereas Le^y (without the nonoate methyl ester) buries approximately 337 Å^2. Like in the binding pocket of BR96, the majority of the residues interacting with the Le^x in 291-2G3-A have an aromatic or polar side chain. In the binding pocket of 291-2G3-A, Trp H33 aromatically stacks with the hydrophobic face of the Gal; in BR96, however, no aromatic stacking with sugar residues is observed. Furthermore, CDR-L2 is not involved in interaction with Le^y, whereas in the 291-2G3-A all CDRs are involved in binding.

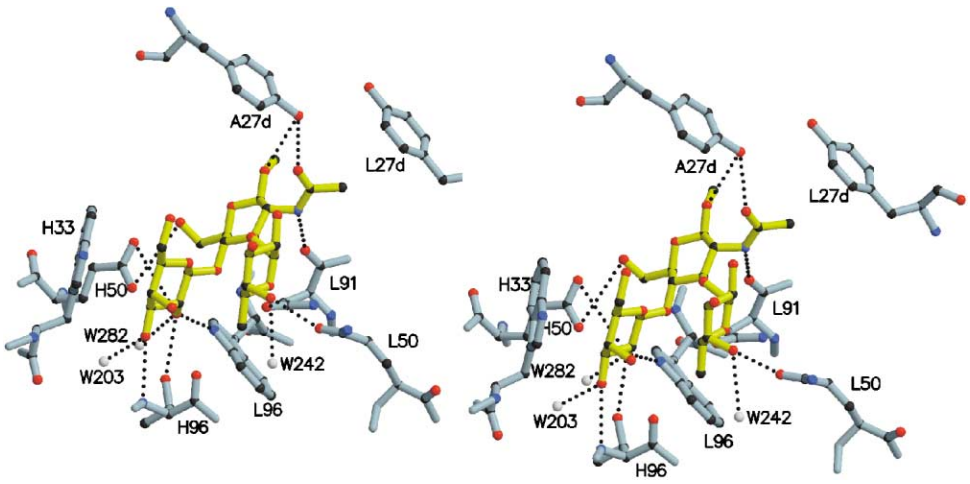

Figure 6. Stereoview of the Binding Site for Le^x

Protein residues and water molecules that are directly interacting with the Le^x trisaccharide are depicted as well as Le^x. The picture was produced with the programs MOLSCRIPT (Kraulis, 1991) and Raster3D (Merritt and Bacon, 1997).

Isothermal Calorimetry

The affinity of 291-2G3-A for Le^x has been determined by isothermal calorimetry (ITC), a sensitive method to determine enthalpy, entropy, and binding constant within one measurement. The thermodynamic parameters for the interaction of 291-2G3-A with Le^x are K_A $9.3 \pm 1 \times 10^4\ M^{-1}$, ΔG -6.7 ± 1.1 kcal mol^{-1}, ΔH -5.0 ± 0.2 kcal mol^{-1}, and $-T\Delta S$ -1.7 ± 0.3 kcal mol^{-1}, with the stoichiometry of the interaction determined to be 1.2. This discrepancy in the stoichiometry of binding is most likely due to the difficulty in accurately determining the actual binding site concentration. Theoretically, this should be two in the case of an antibody-ligand interaction. The fitting of the isotherm was performed with a single binding site model, assuming no cooperativity between the binding sites. Alternative fitting models with multiple sites did not give better results. Both a favorable enthalpy and entropy term contribute to the binding of Le^x to mAb 291-2G3-A, which can be explained by the rather large amount of hydrogen bonds and van der Waals interactions that are formed upon interaction between the protein and all three sugar residues. Usually, no favorable contribution of entropy is observed for protein-ligand associations because of greater motional restrictions for both protein and ligand. An unfavorable change in entropy, however, can be overcome by displacement of solvent from the sugar and/or protein surface (Quiocho, 1989). Most likely, the favorable entropy term of the interaction of Le^x with the antibody stems from solvent displacement realized by the close fit of the sugar at the protein surface. For two structures of bacterial trisaccharides that have been solved previously, the binding affinities have also been measured by ITC. Interestingly, the same range of thermodynamic parameters was found. The thermodynamics of the interaction of a bacterial trisaccharide (Rhaα1-3Rhaα1-3GlcNAcβ-OMe) with mAb SYA/J6 (Vyas et al., 2002) were determined to be K_A 9.5×10^4, ΔG -6.8 kcal mol^{-1}, ΔH -4.3 kcal mol^{-1}, and $-T\Delta S$ -2.5 and for the interaction of *Salmonella* serogroup B O-antigenic trisaccharide epitope (Galα1-2[Abeα1-3]-Manα-OMe) with antibody Se155-4, K_A 1.6×10^5, ΔG -7.3 kcal mol^{-1}, ΔH -4.9 kcal mol^{-1}, and $-T\Delta S$ -2.3 (Bundle et al., 1994; Sigurskjold et al., 1991). Both of these interactions also display a favorable contribution from the entropy term. In analogy with the binding of Le^x to 291-2G3-A, these sugars also display a tight fit on the surface of the Fab fragments.

Basis for the Specificity

Although the affinity of 291-2G3-A for Le^x is not very high, the interaction seems to be very specific. Generally, protein-sugar complexes depend on multivalency to yield an overall higher avidity compared to single-site affinity. To further understand the basis for the specificity of this interaction, a surface plasmon resonance (SPR) study was performed using sugars which are closely related in structure to the Le^x trisaccharide, but lack either the Gal (Fucα1-3GlcNAcβ, FucGlcNAc) or

Table 3. Torsion Angles at the Glycosidic Linkages in Le^x

	Le^x Crystal[a] (ϕ/Ψ)[b]	Le^x Y[c] (ϕ/Ψ)	Le^x C (ϕ/Ψ)	Le$^{y\,d}$ (ϕ/Ψ)
Galβ(1-4)Mag (ϕ1/Ψ1)	−70.5/−107.7	−69.9/−111.1	−66.7/−113.4	−69.8/−103.7
Fucα(1-3)Mag (ϕ2/Ψ2)	−76.7/139.0	−81.4/139.1	−82.7/136.7	−76.7/131.9

[a] Values were taken from one Lewis X molecule from Perez et al. (1996).

[b] Torsion angles at the glycosidic linkages are defined as ϕ1 (O5Gal-C1Gal-O4Mag-C4Mag), Ψ1 (C1Gal-O4Mag-C4Mag-C5Mag), ϕ2 (O5Fuc-C1Fuc-O3Mag-C3Mag), and Ψ2 (C1Fuc-O3Mag-C3Mag-C4Mag).

[c] Torsion angles of the two Le^x molecules present in the unit cell (Y and C) are given.

[d] Values were taken from the BR96-nLe^y structure (PDB code 1CLZ [Jeffrey et al., 1995]).

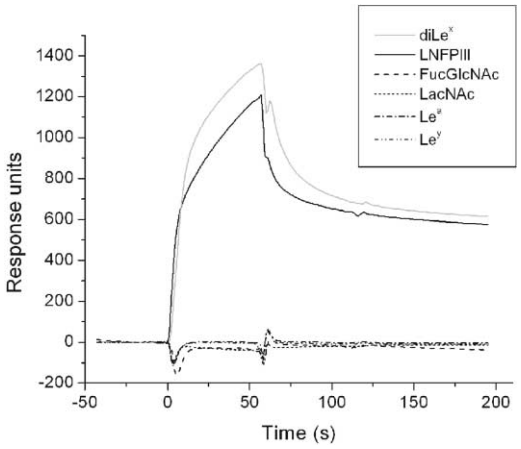

Figure 7. SPR Sensorgram, Binding Pattern of mAb 291-2G3-A with Le^x-Related HSA-Neoglycoconjugates

the Fuc (Galβ1-4GlcNAcβ, LacNAc). Furthermore, the interaction with LewisA (Galβ1-3(Fucα1-4)GlcNAcβ) and LewisY (Fucα1-2Galβ1-4(Fucα1-3)GlcNAcβ, Le^y) was measured. From the SPR sensorgram (Figure 7), it becomes immediately clear that mAb 291-2G3-A does not interact with any of these sugars, confirming its very high specificity for Le^x. All three residues of Le^x form hydrogen bonds with the Fab, explaining why the intact antibody apparently does not interact with the disaccharides lacking a Gal or a Fuc. In the case of Lewis A, modeling studies have shown that the positions of O6 and *N*-Acetyl have interchanged by turning the GlcNAc 180° (Imberty et al., 1995). Most likely, the bulky *N*-Acetyl group would then clash with Glu H50, and several hydrogen bonds will be lost, resulting in no binding of Lewis A to 291-2G3-A. Furthermore, the rather shallow binding pocket encloses the Gal residue, leaving no space for an extra Fuc residue, as is the case for Le^y. By rotating nLe^y from the BR96 complex (PDB code 1CLZ) onto Le^x in the 291-2G3-A structure, it becomes immediately clear that there is no space for the extra Fuc bound to the Gal. mAb 291-2G3-A recognizes both LNFPIII (Galβ1-4(Fucα1-3)GlcNAcβ1-3Galβ1-4Glcβ), a pentasaccharide containing Le^x at its reducing end, and dimeric Le^x (Galβ1-4(Fucα1-3)GlcNAcβ1-3Galβ1-4(Fucα1-3)GlcNAcβ1, diLe^x). Whether mAb 291-2G3-A binds more residues than just the terminal Le^x moiety present in diLe^x, which contains an additional internal Le^x moiety, is difficult to tell from this crystal structure. A crystal structure of the Fab fragment soaked with diLe^x also did not provide a definite answer, as no ligand was bound to the Fab. Most likely, the hapten would clash because of the close proximity in the crystal structure of the binding sites of the two Fabs in the asymmetric unit.

In conclusion, mAb 291-2G3-A is highly specific for Le^x. This specificity is gained by involvement of all six CDRs in the interaction with all three residues from Le^x. A binding pocket is formed that snugly fits the trisaccharide. Higher affinity could possibly be realized by increasing the number of hydrogen bonds between the sugar and the protein. Several residues in the binding pocket could be mutated into amino acids with polar side chains. Improving the hydrogen bonding pattern to the Fuc might increase the affinity, as only one protein residue now interacts with the Fuc. Thr H98, for example, sits rather closely to the Gal and Fuc but is unable to make a hydrogen bond. By mutating this residue into an Arg or a Gln, an extra hydrogen bond might be formed, but this mutation could decrease the stability of the CDR-H3 loop. Another potential amino acid to mutate would be Tyr L32. Its hydroxyl group is now out of range to form a hydrogen bond with O2 of the Fuc; a Gln might be able to make this hydrogen bond. The hydrogen bonding pattern around the Mag and the Gal seems optimized, and therefore, mutations in this area will most likely not increase the affinity.

Recently, an article was published describing the structure and thermodynamics of a peptide carbohydrate-mimic bound to a Fab fragment (Vyas et al., 2003). The use of peptide mimics for carbohydrates could be advantageous, as the synthesis of a short peptide is rather straightforward in contrast with the synthesis of a carbohydrate chain. Furthermore, mimics could be designed that bind the antibody with higher affinity. This new structural information might therefore also aid in the design of a peptide mimic based on Le^x that could be used to improve diagnostics for schistosomiasis or possibly as a research tool to study schistosomiasis or certain cancers.

Experimental Procedures

Monoclonal antibody production, purification, generation of Fab fragments, crystallization, and data collection were carried out as previously described (van Roon et al., 2003). The β-*O*-methyl glycoside of Le^x was chemically synthesized following a route described by Toepfer et al. (1994). An X-ray dataset to 2.05 Å resolution was measured at beamline ID19 at the APS (Argonne, IL) from a crystal without Le^x grown from 25% polyethylene glycol 3350, 0.17 M ammonium sulfate, and 15% glycerol. A crystal grown from 14% PEG 3350, 50 mM Tris (pH 8) was soaked for half an hour with 50 mM Le^x, and an X-ray dataset was measured to 1.8 Å resolution at beamline ID14-1 at the ESRF, Grenoble (France). The data were processed using HKL2000 (Otwinowski and Minor, 1997). Table 1 provides a summary of the data processing statistics.

Structure Determination and Refinement

The structure of the Fab fragments was solved by molecular replacement using the program Molrep (Vagin and Teplyakov, 1997) from the CCP4 program suite (CCP4, 1994). For the native Fab fragment, an anti-LewisY antibody (PDB entry code 1CLZ [Jeffrey et al., 1995]) was used as a search model. Rotation and translation searches were performed for all four monomers in the asymmetric unit at the same time. A solution was found with an R factor of 49.6% and a correlation coefficient of 33.3. Several rounds of rigid body refinement with the program CNS (Brunger et al., 1998) resulted in an R factor of 44.4% for the working set and an R factor of 44.5% for the test set, which contains 5% of randomly chosen reflections. Grouped B value refinement of main chain and side chain atoms using restrained noncrystallographic symmetry (NCS) resulted in an R factor of 33.3% (R_{free} 36.7%). At this stage of the refinement, the correct amino acids were built in manually using Xtalview (Mcree, 1999), omitting loops and side chains that were not visible in the electron density. The refinement was completed using Refmac5 (Murshudov et al., 1997) from the CCP4 package. During refinement, tight NCS restraints were used, and translation, libration, and screw (TLS) parameters were refined (Winn et al., 2001). Both the heavy and the light chains were split up in seven TLS groups, the variable domain was divided in six groups (three containing a CDR loop), and the entire constant domain formed the remaining TLS group.

Water molecules were built automatically, alternated by refinement cycles using ARP/wARP (Lamzin and Wilson, 1993). After the automatic solvent building, water molecules were checked visually and removed if necessary. At the last stage of the refinement, a new version of Refmac5 was used (version 5.2.000), which resulted in an extra drop in R_{free} from 25.5% to 24.3% for the final model. The unliganded Fab model containes 1628 protein residues, 349 water molecules, and 4 sulfate ions.

The structure of the Fab fragment in complex with Le^x was solved by molecular replacement using the native Fab fragment as a search model. A model for the Le^x trisaccharide was obtained by removal of the fucose that was bound to the galactose from a model of LewisY (obtained from PDB entry code 1CLZ [Jeffrey et al., 1995]) and built in the binding site of each Fab fragment at full occupancy. Refinement and addition of water molecules were carried out similarly as described for the native Fab fragment, although in the last stages of the refinement, the 2-fold NCS restraints were removed. The final model contained 826 protein residues, 6 sugar residues, and 288 water molecules having an R_{free} factor of 24.7%. The quality of both models was checked by PROCHECK (Laskowski et al., 1993) and WHATIF (Vriend, 1990). Crystallographic statistics are included in Table 1.

Neoglycoconjugates

The human serum albumin (HSA) Lewis neoglycoconjugates, HSA-LNFPIII, HSA-dimeric Le^x, HSA-LewisY, and HSA-LewisA, Isosep (Tullinge, Sweden) were a kind gift of Dr. B. Appelmelk (Amsterdam, The Netherlands). These neoglycoconjugates contained on average 22 mol sugar per mol HSA. HSA-LacNAc and HSA-FucGlcNAc were synthesized following the route as described by Toepfer et al. (1994). These neoglycoconjugates contained on average 7–10 mol sugar per mol HSA.

Surface Plasmon Resonance Analysis of Binding of 291-2G3-A with Lewis-type Neoglycoconjugates

A qualitative study of the binding of mAbs with Lewis-type neoglycoconjugates was carried out using surface plasmon resonance (SPR). The Biacore 3000 instrument, CM5 sensor chips, and an amino coupling kit were purchased from Biacore AB (Uppsala, Sweden). All buffers were filtered and degassed under vacuum before use. Immobilization of the neoglycoconjugates was performed using the standard amino coupling procedure according to the instructions of the manufacturer at a flow rate of 5 μl/min. In short, the carboxymethylated surface of the CM5 sensor chip was activated by a 7 min pulse of a 1:1 mixture of 0.1 M *N*-hydroxysuccinimide and 0.1 M *N*-Ethyl-*N*′-(dimethylaminopropyl)carbodiimide, followed by several injections of the neoglycoconjugate at a concentration of 25 μg/ml in 10 mM sodium acetate (pH 4.5) until the desired level of immobilization was achieved. The Le^x neoglycoconjugates were immobilized to a level of 7500 RU. After immobilization, unreacted groups were blocked by the injection of 300 μl 1 M ethanolamine-HCl (pH 8.5). Unmodified HSA was coupled on one flow channel of each sensor chip as a control. All analyses were performed at a flow rate of 5 μl/min using HEPES buffered saline (pH 7.4) containing 3 mM EDTA and 0.005% surfactant P20 (HBS-EP) as eluent. Five microliters of purified 291-2G3-A (1 mg/ml in 0.035 M phosphate-buffered saline [PBS]) was injected. After subtraction of the response units of the HSA control channel, the interaction of the antibody was interpreted as binding (+) or not binding (−) with all HSA-neoglycoconjugates. The surface was regenerated with 5 μl 25 mM HCl.

SPR Data Analysis

The data were analyzed using the BIA evaluation software (version 3.0). We corrected for the refractive index change and nonspecific binding by using the HSA control surface as a blank.

Isothermal Calorimetry

ITC was measured using the VP-ITC MicroCalorimeter, Microcal LLC (Northampton, MA). Protein A purified antibody was dialyzed against PBS and concentrated using an Ultrafree-4 Centrifugal Filter Unit with a cutoff of 10 kDa (Millipore). The protein concentration was determined spectrophotometrically, using a calculated extinction coefficient of 1.63 $mg^{-1}ml$ (Gill and Vonhippel, 1989). Le^x was purchased as a dry powder from Toronto Research Chemicals (North York, ON, Canada). Both protein and trisaccharide were dissolved in the same buffer. The protein solution used had a starting concentration of 44 μM, and the starting ligand concentration was 1.8 mM. The titrations were carried out at 22°C by 5, 10, or 12 s injections of ligand into the protein solution. Three measurements using different concentrations of protein and ligand were performed. For a typical measurement, see Supplemental Figure S1 in the supplemental information at http://www.structure.org/cgi/content/full/12/7/1227/DC1. Titration of ligand into buffer was used as a control to correct for the released background heat. The measurements were analyzed by the ORIGIN software package (Microcal, LLC), and the data were processed using the One Site binding model assuming there is no cooperativity between the sites. The stated values and standard deviations are derived from data from three measurements.

Sequencing of Variable Domains

Standard molecular biology protocols were used throughout the procedure. Hybridoma cells (10^6 cells) were sedimented by centrifugation at 300 × g in 5 min at room temperature. Total mRNA was isolated with the Oligotex Direct micro mRNA isolation system (Qiagen Inc.) according to the protocol of the manufacturer. The cell lysates were homogenized using a 20-gauge syringe; the purified mRNA was eventually eluted in 100 μl elution solution. The mRNA was used as templates for the synthesis of cDNA of the IgG variable regions of the hybridoma cells. cDNA synthesis and amplification of the synthesized cDNA was performed in one step according to the Titan One Tube RT-PCR System (Roche, Basel, Switzerland). The primers used were obtained from the Mouse Ig-Primer set of the Ig-Prime System (Novagen); for primer sequences, see the protocol. Primer sets $MuIgV_H5'$-F and $MuIgGV_H3'$-2 were used for the 5′ and 3′ ends of heavy chains, respectively. Primer sets $MuIg_\kappa V_L5'$-F and $MuIg\kappa V_L3'$-1 were used for the 5′ and 3′ ends of the light chains, respectively. Each reaction was performed with 4 μl mRNA solution. The reaction was started by incubation at 50°C for 30 min for the synthesis of cDNA. The amplification was performed at 94°C for 2 min, followed by 35 cycles of 1 min at 94°C, 1 min at 60°C, and 2 min at 72°C followed by a final extension period of 6 min at 72°C. PCR reaction solutions were screened for DNA fragments of approximately 140 bp with electrophoresis using a 1% agarose gel. Reaction solutions containing DNA fragments were extracted with one volume of a chloroform:isoamyl-alcohol (24:1) solution. The fragments were cloned in the pSTBlue-1 cloning vector according to the protocol of the Perfectly Blunt Cloning Kit (Novagen) and transformed into NovaBlue singles competent cells. Transformants were selected for the kanamycin resistance marker of the cloning vector and for the vector carrying an insert with X-Gal (5-bromo-4chloro-3indolyl-β-galactopyranoside). Sequences were obtained commercially (Base Clear, Leiden, The Netherlands) by automated dideoxy chain-termination technology using the T7 and SP6 promoter primers.

Acknowledgments

We would like to thank Dr. Mark Hilge (Nijmegen, The Netherlands) for helpful discussions. We are very grateful to Dr. Patrick Celie from The Netherlands Cancer Institute (Amsterdam, The Netherlands) for assisting with the ITC measurements. We also thank Mr. René van Zeyl for the supply of large quantities of mAb 291-2G3-A and Dr. Ben Appelmelk for the kind gift of the HSA-neoglycoconjugates. We are thankful for the support of Dr. Norma Duke of the APS at Argonne (IL) during data collection. Use of the Argonne National Laboratory Structural Biology Center beamlines at the Advanced Photon Source was supported by the U.S. Department of Energy, Office of Energy Research, under contract No. W-31-109-ENG-38. Furthermore, we acknowledge the European Synchrotron Radiation Facility at Grenoble, France, for provision of synchrotron radiation facilities, and we would like to thank Dr. Pierre Legrand for assistance in using beamline ID 14-1.

Received: February 17, 2004
Revised: April 28, 2004
Accepted: May 2, 2004
Published: July 13, 2004

References

Borojevic, R., Santos-da-Silva, C., and Carvalho, E.A. (1983). Chronic schistosomiasis mansoni: splenic myelopoiesis and inhibition of neutrophil granulocytopoiesis mediated by the sera of patients. J. Infect. Dis. *148*, 422–426.

Brunger, A.T., Adams, P.D., Clore, G.M., Delano, W.L., Gros, P., Grosse-Kunstleve, R.W., Jiang, J.S., Kuszewski, J., Nilges, M., Pannu, N.S., et al. (1998). Crystallography & NMR system: a new software suite for macromolecular structure determination. Acta Crystallogr. D Biol. Crystallogr. *54*, 905–921.

Bundle, D.R., Eichler, E., Gidney, M.A.J., Meldal, M., Ragauskas, A., Sigurskjold, B.W., Sinnott, B., Watson, D.C., Yaguchi, M., and Young, N.M. (1994). Molecular recognition of a Salmonella trisaccharide epitope by monoclonal-antibody Se155–4. Biochemistry *33*, 5172–5182.

Calarese, D.A., Scanlan, C.N., Zwick, M.B., Deechongkit, S., Mimura, Y., Kunert, R., Zhu, P., Wormald, M.R., Stanfield, R.L., Roux, K.H., et al. (2003). Antibody domain exchange is an immunological solution to carbohydrate cluster recognition. Science *300*, 2065–2071.

CCP4 (Collaborative Computational Project 4) (1994). The CCP4 suite: programs for protein crystallography. Acta Crystallogr. D Biol. Crystallogr. *50*, 760–763.

Cygler, M., Rose, D.R., and Bundle, D.R. (1991). Recognition of a cell-surface oligosaccharide of pathogenic Salmonella by an antibody Fab fragment. Science *253*, 442–445.

De Jonge, N., Kremsner, P.G., Krijger, F.W., Schommer, G., Fillie, Y.E., Kornelis, D., van Zeyl, R.J., Van Dam, G.J., Feldmeier, H., and Deelder, A.M. (1990). Detection of the schistosome circulating cathodic antigen by enzyme immunoassay using biotinylated monoclonal antibodies. Trans. R. Soc. Trop. Med. Hyg. *84*, 815–818.

Fox, N., Damjanov, I., Knowles, B.B., and Solter, D. (1983). Immunohistochemical localization of the mouse stage-specific embryonic antigen 1 in human tissues and tumors. Cancer Res. *43*, 669–678.

Gill, S.C., and Vonhippel, P.H. (1989). Calculation of protein extinction coefficients from amino-acid sequence data. Anal. Biochem. *182*, 319–326.

Hakomori, S. (1984). Tumor-associated carbohydrate antigens. Annu. Rev. Immunol. *2*, 103–126.

Hakomori, S. (2000). Traveling for the glycosphingolipid path. Glycoconj. J. *17*, 627–647.

Hellstrom, I., Garrigues, H.J., Garrigues, U., and Hellstrom, K.E. (1990). Highly tumor-reactive, internalizing, mouse monoclonal-antibodies to Ley-related cell-surface antigens. Cancer Res. *50*, 2183–2190.

Hokke, C.H., and Deelder, A.M. (2001). Schistosome glycoconjugates in host-parasite interplay. Glycoconj. J. *18*, 573–587.

Huang, H.H., Tsai, P.L., and Khoo, K.H. (2001). Selective expression of different fucosylated epitopes on two distinct sets of *Schistosoma mansoni* cercarial O-glycans: identification of a novel core type and Lewis X structure. Glycobiology *11*, 395–406.

Imberty, A., Mikros, E., Koca, J., Mollicone, R., Oriol, R., and Perez, S. (1995). Computer-simulation of histo-blood group oligosaccharides—energy maps of all constituting disaccharides and potential-energy surfaces of 14 Abh and Lewis carbohydrate antigens. Glycoconj. J. *12*, 331–349.

Jeffrey, P.D., Bajorath, J., Chang, C.Y., Yelton, D., Hellstrom, I., Hellstrom, K.E., and Sheriff, S. (1995). The X-ray structure of an antitumor antibody in complex with antigen. Nat. Struct. Biol. *2*, 466–471.

Khoo, K.H., Huang, H.H., and Lee, K.M. (2001). Characteristic structural features of schistosome cercarial N-glycans: expression of Lewis X and core xylosylation. Glycobiology *11*, 149–163.

Koster, B., and Strand, M. (1994). *Schistosoma mansoni*: immunolocalization of two different fucose-containing carbohydrate epitopes. Parasitology *108*, 433–446.

Kraulis, P.J. (1991). Molscript a program to produce both detailed and schematic plots of protein structures. J. Appl. Crystallogr. *24*, 946–950.

Lamzin, V.S., and Wilson, K.S. (1993). Automated refinement of protein models. Acta Crystallogr. D Biol. Crystallogr. *49*, 129–147.

Laskowski, R.A., Macarthur, M.W., Moss, D.S., and Thornton, J.M. (1993). Procheck—a program to check the stereochemical quality of protein structures. J. Appl. Crystallogr. *26*, 283–291.

Martin, A.C.R. (1996). Accessing the Kabat antibody sequence database by computer. Proteins *25*, 130–133.

Mcree, D.E. (1999). XtalView Xfit—a versatile program for manipulating atomic coordinates and electron density. J. Struct. Biol. *125*, 156–165.

Merritt, E.A., and Bacon, D.J. (1997). Raster3D: photorealistic molecular graphics. Methods Enzymol. *277*, 505–524.

Morea, V., Tramontano, A., Rustici, M., Chothia, C., and Lesk, A.M. (1998). Conformations of the third hypervariable region in the VH domain of immunoglobulins. J. Mol. Biol. *275*, 269–294.

Murshudov, G.N., Vagin, A.A., and Dodson, E.J. (1997). Refinement of macromolecular structures by the maximum-likelihood method. Acta Crystallogr. D Biol. Crystallogr. *53*, 240–255.

Nguyen, H.P., Seto, N.O.L., Mackenzie, C.R., Brade, L., Kosma, P., Brade, H., and Evans, S.V. (2003). Germline antibody recognition of distinct carbohydrate epitopes. Nat. Struct. Biol. *10*, 1019–1025.

Nicholls, A., Sharp, K.A., and Honig, B. (1991). Protein Folding and association—insights from the interfacial and thermodynamic properties of hydrocarbons. Proteins *11*, 281–296.

Nyame, A.K., Pilcher, J.B., Tsang, V.C., and Cummings, R.D. (1996). Schistosoma mansoni infection in humans and primates induces cytolytic antibodies to surface Le(x) determinants on myeloid cells. Exp. Parasitol. *82*, 191–200.

Nyame, A.K., Pilcher, J.B., Tsang, V.C., and Cummings, R.D. (1997). Rodents infected with Schistosoma mansoni produce cytolytic IgG and IgM antibodies to the Lewis x antigen. Glycobiology *7*, 207–215.

Otwinowski, Z., and Minor, W. (1997). Processing of X-ray diffraction data collected in oscillation mode. Methods Enzymol. *276*, 307–326.

Padlan, E.A., and Kabat, E.A. (1991). Modeling of antibody combining sites. Methods Enzymol. *203*, 3–21.

Perez, S., MouhousRiou, N., Nifantev, N.E., Tsvetkov, Y.E., Bachet, B., and Imberty, A. (1996). Crystal and molecular structure of a histo-blood group antigen involved in cell adhesion: the Lewis x trisaccharide. Glycobiology *6*, 537–542.

Quiocho, F.A. (1989). Protein-carbohydrate interactions—basic molecular-features. Pure Appl. Chem. *61*, 1293–1306.

Richter, D., Incani, R.N., and Harn, D.A. (1996). Lacto-N-fucopentaose III (Lewis x), a target of the antibody response in mice vaccinated with irradiated cercariae of Schistosoma mansoni. Infect. Immun. *64*, 1826–1831.

Shirai, H., Kidera, A., and Nakamura, H. (1996). Structural classification of CDR-H3 in antibodies. FEBS Lett. *399*, 1–8.

Shirai, H., Kidera, A., and Nakamura, N. (1999). H3-rules: identification of CDR-H3 structures in antibodies. FEBS Lett. *455*, 188–197.

Sigurskjold, B.W., Altman, E., and Bundle, D.R. (1991). Sensitive titration microcalorimetric study of the binding of Salmonella O-antigenic oligosaccharides by a monoclonal-antibody. Eur. J. Biochem. *197*, 239–246.

Srivatsan, J., Smith, D.F., and Cummings, R.D. (1992). The human blood fluke *Schistosoma mansoni* synthesizes glycoproteins containing the Lewis X antigen. J. Biol. Chem. *267*, 20196–20203.

Toepfer, A., Kinzy, W., and Schmidt, R.R. (1994). Efficient synthesis of the Lewis antigen-X (Le(X)) family. Liebigs Ann. Chem. *65*, 449–464.

Vagin, A., and Teplyakov, A. (1997). MOLREP: an automated program for molecular replacement. J. Appl. Crystallogr. *30*, 1022–1025.

Van Dam, G.J., Bergwerff, A.A., Thomas-Oates, J.E., Rotmans, J.P., Kamerling, J.P., Vliegenthart, J.F., and Deelder, A.M. (1994). The

immunologically reactive O-linked polysaccharide chains derived from circulating cathodic antigen isolated from the human blood fluke Schistosoma mansoni have Lewis x as repeating unit. Eur. J. Biochem. *225*, 467–482.

Van Dam, G.J., Claas, F.H., Yazdanbakhsh, M., Kruize, Y.C., van Keulen, A.C., Ferreira, S.T., Rotmans, J.P., and Deelder, A.M. (1996). Schistosoma mansoni excretory circulating cathodic antigen shares Lewis-x epitopes with a human granulocyte surface antigen and evokes host antibodies mediating complement-dependent lysis of granulocytes. Blood *88*, 4246–4251.

Van Remoortere, A., Hokke, C.H., Van Dam, G.J., van Die, I, Deelder, A.M., and van den Eijnden, D.H. (2000). Various stages of schistosoma express Lewis(x), LacdiNAc, GalNAcbeta1-4 (Fucalpha1-3) GlcNAc and GalNAcbeta1-4(Fucalpha1-2Fucalpha1-3)GlcNAc carbohydrate epitopes: detection with monoclonal antibodies that are characterized by enzymatically synthesized neoglycoproteins. Glycobiology *10*, 601–609.

Van Remoortere, A., Van Dam, G.J., Hokke, C.H., van den Eijnden, D.H., van, Die, I, and Deelder, A.M. (2001). Profiles of immunoglobulin M (IgM) and IgG antibodies against defined carbohydrate epitopes in sera of Schistosoma-infected individuals determined by surface plasmon resonance. Infect. Immun. *69*, 2396–2401.

Van Remoortere, A., Vermeer, H.J., Van Roon, A.M., Langermans, J.A., Thomas, A.W., Wilson, R.A., van Die, I., van den Eijnden, D.H., Agoston, K., Kerekgyarto, J., et al. (2003). Dominant antibody responses to Fuc alpha 1–3GalNAc and Fuc alpha 1–2Fuc alpha 1–3GlcNAc containing carbohydrate epitopes in Pan troglodytes vaccinated and infected with Schistosoma mansoni. Exp. Parasitol. *105*, 219–225.

van Roon, A.M.M., Pannu, N.S., Hokke, C.H., Deelder, A.M., and Abrahams, J.P. (2003). Crystallization and preliminary X-ray analysis of an anti-LewisX Fab fragment with and without its LewisX antigen. Acta Crystallogr. D Biol. Crystallogr. *59*, 1306–1309.

van Roon, A.M.M., Van de Vijver, K.K., Jacobs, W., Van Marck, E.A., van Dam, G.J., Hokke, C.H., and Deelder, A.M. (2004). Discrimination between the anti-monomeric and the anti-multimeric Lewis X response in murine Schistosomiasis. Microbes Infect., in press.

Velupillai, P., dos Reis, E.A., dos Reis, M.G., and Harn, D.A. (2000). Lewis(x)-containing oligosaccharide attenuates schistosome egg antigen- induced immune depression in human schistosomiasis. Hum. Immunol. *61*, 225–232.

Velupillai, P., and Harn, D.A. (1994). Oligosaccharide-specific induction of interleukin 10 production by $B220^{+}$ cells from schistosome-infected mice: a mechanism for regulation of $CD4^{+}$ T-cell subsets. Proc. Natl. Acad. Sci. USA *91*, 18–22.

Villeneuve, S., Souchon, H., Riottot, M.M., Mazie, J.C., Lei, P., Glaudemans, C.P.J., Kovac, P., Fournier, J.M., and Alzari, P.M. (2000). Crystal structure of an anti-carbohydrate antibody directed against Vibrio cholerae 01 in complex with antigen: molecular basis for serotype specificity. Proc. Natl. Acad. Sci. USA *97*, 8433–8438.

Vriend, G. (1990). What If—a molecular modeling and drug design program. J. Mol. Graph. *8*, 52.

Vyas, N.K., Vyas, M.N., Chervenak, M.C., Johnson, M.A., Pinto, B.M., Bundle, D.R., and Quiocho, F.A. (2002). Molecular recognition of oligosaccharide epitopes by a monoclonal fab specific for Shigella flexneri Y lipopolysaccharide: X-ray structures and thermodynamics. Biochemistry *41*, 13575–13586.

Vyas, N.K., Vyas, M.N., Chervenak, M.C., Bundle, D.R., Pinto, B.M., and Quiocho, F.A. (2003). Structural basis of peptide-carbohydrate mimicry in an antibody-combining site. Proc. Natl. Acad. Sci. USA *100*, 15023–15028.

Weiss, J.B., and Strand, M. (1985). Characterization of developmentally regulated epitopes of egg glycoprotein antigens. J. Immunol. *135*, 1421–1429.

Wilson, I.A., and Stanfield, R.L. (1993). Antibody-antigen interactions. Curr. Opin. Struct. Biol. *3*, 113–118.

Winn, M.D., Isupov, M.N., and Murshudov, G.N. (2001). Use of TLS parameters to model anisotropic displacements in macromolecular refinement. Acta Crystallogr. D Biol. Crystallogr. *57*, 122–133.

Wormald, M.R., Petrescu, A.J., Pao, Y.L., Glithero, A., Elliott, T., and Dwek, R.A. (2002). Conformational studies of oligosaccharides and glycopeptides: complementarity of NMR, X-ray crystallography, and molecular modelling. Chem. Rev. *102*, 371–386.

Wuhrer, M., Dennis, R.D., Doenhoff, M.J., Lochnit, G., and Geyer, R. (2000). Schistosoma mansoni cercarial glycolipids are dominated by Lewis X and pseudo-Lewis Y structures. Glycobiology *10*, 89–101.

Zdanov, A., Li, Y., Bundle, D.R., Deng, S.J., Mackenzie, C.R., Narang, S.A., Young, N.M., and Cygler, M. (1994). Structure of a single-chain antibody variable domain (Fv) fragment complexed with a carbohydrate antigen at 1.7-angstrom resolution. Proc. Natl. Acad. Sci. USA *91*, 6423–6427.

Accession Numbers

Data for Fab fragment 291-2G3-A uncomplexed and complexed with Lewis X were deposited with the PDB under codes 1UZ6 and 1UZ8, respectively.